Ergodic properties of fractional Brownian-Langevin motion

Weihua Deng[1,2] and Eli Barkai[1]
[1]*Department of Physics, Bar Ilan University, Ramat-Gan 52900, Israel*
[2]*School of Mathematics and Statistics, Lanzhou University, Lanzhou 730000, People's Republic of China*
(Received 15 September 2008; published 13 January 2009)

We investigate the time average mean-square displacement $\overline{\delta^2}(x(t))=\int_0^{t-\Delta}[x(t'+\Delta)-x(t')]^2dt'/(t-\Delta)$ for fractional Brownian-Langevin motion where $x(t)$ is the stochastic trajectory and Δ is the lag time. Unlike the previously investigated continuous-time random-walk model, $\overline{\delta^2}$ converges to the ensemble average $\langle x^2\rangle \sim t^{2H}$ in the long measurement time limit. The convergence to ergodic behavior is slow, however, and surprisingly the Hurst exponent $H=\frac{3}{4}$ marks the critical point of the speed of convergence. When $H<\frac{3}{4}$, the ergodicity breaking parameter $E_B=[\langle[\overline{\delta^2}(x(t))]^2\rangle-\langle\overline{\delta^2}(x(t))\rangle^2]/\langle\overline{\delta^2}(x(t))\rangle^2\sim k(H)\Delta t^{-1}$, when $H=\frac{3}{4}$, $E_B\sim(\frac{9}{16})(\ln t)\Delta t^{-1}$, and when $\frac{3}{4}<H<1$, $E_B\sim k(H)\Delta^{4-4H}t^{4H-4}$. In the ballistic limit $H\to 1$ ergodicity is broken and $E_B\sim 2$. The critical point $H=\frac{3}{4}$ is marked by the divergence of the coefficient $k(H)$. Fractional Brownian motion as a model for recent experiments of subdiffusion of mRNA in the cell is briefly discussed, and a comparison with the continuous-time random-walk model is made.

DOI: 10.1103/PhysRevE.79.011112 PACS number(s): 02.50.−r, 05.30.Pr, 05.40.−a, 05.10.Gg

I. INTRODUCTION

Fractional calculus, e.g., $d^{1/2}/dt^{1/2}$, is a powerful mathematical tool for the investigation of physical and biological phenomena with long-range correlations or long memory [1]. For example, fractional calculus describes the mechanical memory of viscoelastic materials [2]. An important application of fractional calculus is the stochastic modeling of anomalous diffusion. Fractional Fokker-Planck equations describe the long time behavior of the continuous-time random walk (CTRW) model, when waiting times and/or jump lengths have power-law distributions [1,3–5]. A different stochastic approach to anomalous diffusion is based on fractional Brownian motion (fBM) [6], which is related to recently investigated fractional Langevin equations (see details below) [7–10].

Recent single-particle tracking of mRNA molecules [11] and lipid granules [12] in living cells revealed that time-averaged mean-square displacement $\overline{\delta^2}$ (defined below more precisely) of individual particles remains a random variable while indicating that the particle motion is subdiffusive. This means that the time averages are not identical to ensemble averages. Such breaking of ergodicity was investigated within the subdiffusive CTRW model [13,14]. It was shown that transport and diffusion constants extracted from single-particle trajectories remain random variables, even in the long measurement time limit. For a nontechnical point of view on this problem, see [15]. Here we consider the fluctuations of the time-averaged mean-square displacement

$$\overline{\delta^2}(x(t))=\frac{\int_0^{t-\Delta}[x(t'+\Delta)-x(t')]^2dt'}{t-\Delta}, \tag{1}$$

where Δ is called the lag time, and $x(t)$ is the stochastic path of fBM or fractional Langevin motion. As is well known, if $x(t)$ is normal Brownian motion, the ensemble average mean-square displacement is $\langle x^2(t)\rangle=2D_1t$ while the time-average mean-square displacement of the single trajectory $\overline{\delta^2}(x(t))=2D_1\Delta$ in statistical sense and in the long measurement time limit. Hence in experiments we may use a single trajectory of a Brownian particle to estimate the diffusion constant D_1. Will similar ergodic behavior be found also for fBM and fractional Langevin equations? Or will fBM exhibit ergodicity breaking similar to the CTRW model? Note that the problem of estimating diffusion constants from single-particle tracking, for normal diffusion, is already well investigated [16].

In recent years, there was much interest in nonergodicity of anomalous diffusion processes. A well investigated system is blinking quantum dots [17,18], which exhibit a Lévy walk type of dynamics (a superdiffusive process). A very general formula for the distribution of time averages for weakly nonergodic systems was derived in [19], and this framework was shown to describe the subdiffusive CTRW [20]. Bao *et al.* have investigated ergodicity breaking for stochastic dynamics described by the generalized Langevin equation [21]. They considered the time-averaged velocity variance. The latter converges to k_BT/m in thermal equilibrium if the process is ergodic. It was shown [21] that under certain conditions, the generalized Langevin equation is nonergodic (see also [22–26]). Our work, following the recent experiments [11,12], considers the time average of the mean-square displacements, which yields information on diffusion constants.

This paper is organized as follows. In Sec. II, we define the models under investigation: fBM and overdamped and underdamped fractional Langevin motion. In Sec. III, we derive the ergodic properties of the models under investigation, in particular we analyze the fluctuations of the time average Eq. (1). The technical parts of our derivation and simulation procedure are left for Appendixes A and B. Finally, we end with a discussion in Sec. IV, where comparison to the CTRW model is made, and the relation with experiments is mentioned very briefly.

II. STOCHASTIC MODELS

A. Fractional Brownian motion

Fractional Brownian motion is generated from fractional Gaussian noise, like Brownian motion from white noise.

Mandelbrot and van Ness [6] defined fBM with

$$B_H(t) := \frac{1}{\Gamma\left(H+\frac{1}{2}\right)}\left(\int_0^t (t-\tau)^{H-(1/2)}dB(\tau) + \int_{-\infty}^0 [(t-\tau)^{H-(1/2)} - (-\tau)^{H-(1/2)}]dB(\tau)\right), \quad (2)$$

where Γ represents the Gamma function and $0<H<1$ is called the Hurst parameter. The integrator B is ordinary Brownian motion. Note that B is recovered when taking $H=\frac{1}{2}$. The right-hand side of Eq. (2) is the sum of two Gaussian processes. In the definition, for the first Gaussian process, we identify the so-called fBM of Riemann-Liouville type [27]. Standard fBM, i.e., Eq. (2), is the only Gaussian self-similar process with stationary increments [6]. The variance of $B_H(t)$ is $2D_Ht^{2H}$, where $D_H=[\Gamma(1-2H)\cos(H\pi)]/(2H\pi)$. In the following, for some given H, we denote the trajectory sample of fBM $x(t)$. The properties that uniquely characterize the fBM can be summarized as follows: $x(t)$ has stationary increments; $x(0)=0$ and $\langle x(t)\rangle=0$ for $t\geq 0$; $\langle x^2(t)\rangle=2D_Ht^{2H}$ for $t\geq 0$; $x(t)$ has a Gaussian distribution for $t>0$. From the above properties, the covariance function is [28]

$$\langle x(t_1)x(t_2)\rangle = D_H(t_1^{2H} + t_2^{2H} - |t_1-t_2|^{2H}), \quad t_1,t_2 > 0. \quad (3)$$

The nonindependent increment process of fBM, called fractional Gaussian noise (fGn), is given by

$$\xi(t) = \frac{dx(t)}{dt}, \quad t > 0, \quad (4)$$

which is a stationary Gaussian process and has a standard normal distribution for any $t>0$. The mean $\langle\xi(t)\rangle=0$ and the covariance is

$$\langle\xi(t_1)\xi(t_2)\rangle = 2D_HH(2H-1)|t_1-t_2|^{2H-2}, \quad t_1,t_2 > 0. \quad (5)$$

B. Fractional Langevin equation

The standard Langevin equation with white noise can be extended to a generalized Langevin equation with a power-law memory kernel. Such an approach was recently used to model the dynamics of single proteins by the Xie group [8] and can be derived from the Kac-Zwanzig model of Brownian motion [29]. The underdamped fractional Langevin equation reads

$$m\frac{d^2y(t)}{dt^2} = -\bar{\gamma}\int_0^t (t-\tau)^{2H-2}\frac{dy}{d\tau}d\tau + \eta\xi(t), \quad (6)$$

where according to the fluctuation dissipation theorem

$$\eta = \sqrt{\frac{k_BT\bar{\gamma}}{2D_HH(2H-1)}},$$

$\xi(t)$ is fGn defined in Eqs. (4) and (5), $\frac{1}{2}<H<1$ is the Hurst parameter, and $\bar{\gamma}>0$ is a generalized friction constant. Equation (5) is called a fractional Langevin equation since the memory kernel yields a fractional derivative of the velocity (use the Laplace transform or see [1,30]). Note that if $0<H<\frac{1}{2}$, the integral over the memory kernel diverges, and hence it is assumed that $\frac{1}{2}<H<1$. This leads to subdiffusive behavior $\langle y^2\rangle \sim t^{2-2H}$. An overdamped fractional Langevin equation, where Newton's acceleration term is neglected, reads [8]

$$0 = -\bar{\gamma}\int_0^t (t-\tau)^{2H-2}\frac{dz}{d\tau}d\tau + \eta\xi(t). \quad (7)$$

Another convenient way to write Eq. (6) is

$$m\frac{d^2y(t)}{dt^2} = -\bar{\gamma}\Gamma(2H-1)\frac{d^{2-2H}y(t)}{dt^{2-2H}} + \eta\xi(t), \quad (8)$$

where the fractional derivative is defined in the Caputo sense,

$$\frac{d^{2-2H}y(t)}{dt^{2-2H}} = \frac{1}{\Gamma(2H-1)}\int_0^t (t-\tau)^{2H-2}\frac{dy}{d\tau}d\tau. \quad (9)$$

In recent years, fractional calculus was used to describe many physical systems [1]. In what follows, we investigate ergodic properties of the processes $x(t)$, $y(t)$, and $z(t)$.

III. ERGODIC PROPERTIES

In this section, we consider the fluctuations of time-average mean-square displacement $\overline{\delta^2}$ for three models of anomalous diffusion. If the average of $\overline{\delta^2}$ is equal to the ensemble average $\langle x^2\rangle$, and if the variance of $\overline{\delta^2}$ tends to zero when the measurement time is long, the process is ergodic, since then the distribution of $\overline{\delta^2}$ tends to a delta function centered on the ensemble average. Hence the variance of $\overline{\delta^2}$ is a measure of ergodicity breaking.

A. Fractional Brownian motion

For fBM, using Eqs. (1) and (3),

$$\langle\overline{\delta^2}(x(t))\rangle = \frac{\int_0^{t-\Delta}\langle[x(t'+\Delta)-x(t')]^2\rangle dt'}{t-\Delta} = 2D_H\Delta^{2H}, \quad (10)$$

hence $\langle\overline{\delta^2}\rangle=\langle x^2\rangle$ for all times. The variance of $\overline{\delta^2}(x(t))$ is

$$X_{\text{var}}[\overline{\delta^2}(x(t))] = \langle[\overline{\delta^2}(x(t))]^2\rangle - \langle\overline{\delta^2}(x(t))\rangle^2. \quad (11)$$

A dimensionless measure of ergodicity breaking (E_B) is the parameter

$$E_B(x(t)) = \frac{X_{\text{var}}[\overline{\delta^2}(x(t))]}{\langle\overline{\delta^2}(x(t))\rangle^2}, \quad (12)$$

which is zero in the limit $t\to\infty$ if the process is ergodic. In Appendix A, we derive our main result. Valid for large t, we find

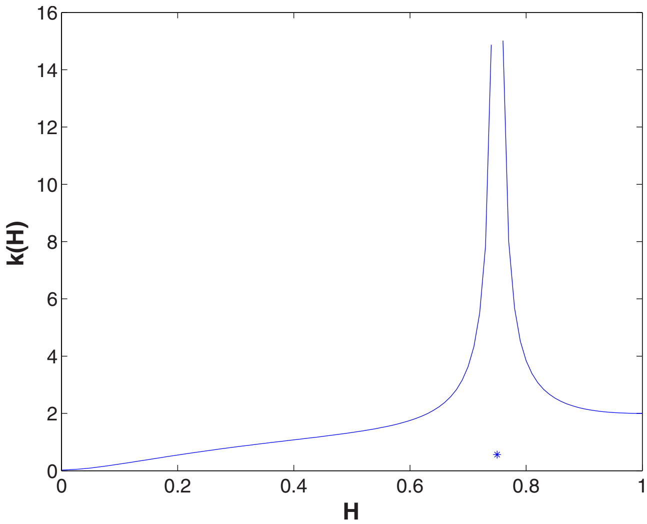

FIG. 1. (Color online) The function of $k(H)$, Eq. (14).

$$E_B(x(t)) \sim \begin{cases} k(H)\dfrac{\Delta}{t}, & 0 < H < \dfrac{3}{4}, \\ k(H)\dfrac{\Delta}{t}\ln t, & H = \dfrac{3}{4}, \\ k(H)\left(\dfrac{\Delta}{t}\right)^{4-4H}, & \dfrac{3}{4} < H < 1, \end{cases} \tag{13}$$

where

$$k(H) = \begin{cases} \displaystyle\int_0^\infty [(\tau+1)^{2H} + |\tau-1|^{2H} - 2\tau^{2H}]^2 d\tau, & 0 < H < \dfrac{3}{4}, \\ 4H^2(2H-1)^2 = \dfrac{9}{16}, & H = \dfrac{3}{4}, \\ \left(\dfrac{4}{4H-3} - \dfrac{4}{4H-2}\right)H^2(2H-1)^2, & \dfrac{3}{4} < H < 1. \end{cases} \tag{14}$$

The most remarkable result is that $k(H)$ diverges when $H \to \frac{3}{4}$, $H=\frac{3}{4}$ marks a nonsmooth transition in the properties of fractional Brownian motion; see Fig. 1. Notice that $k(H) \to 0$ when $H \to 0$ so the asymptotic convergence is expected to hold only after very long times when H is small, since then the diffusion process is very slow. When $H \to 1$, we have $E_B[x(t)] \sim 2$ indicating ergodicity breaking; see Fig. 2.

Figure 3 displays the simulations of $\overline{\delta^2}(x(t))$ showing the randomness of the time average for finite-time measurements. In this simulation, we generate single trajectories using Hosking's method [34], and then perform the time average to find $\overline{\delta^2}$. The figure mimics the experimental results on single lipid granule in a yeast cell and of mRNA molecules inside living E-coli cells [11,12], where $H=\frac{3}{8}$ was recorded. Note, however, that the scatter of the experiments data seems larger (see figures in [11,12]), at least with the naked eye. Further, we did not consider in our simulations the effect of

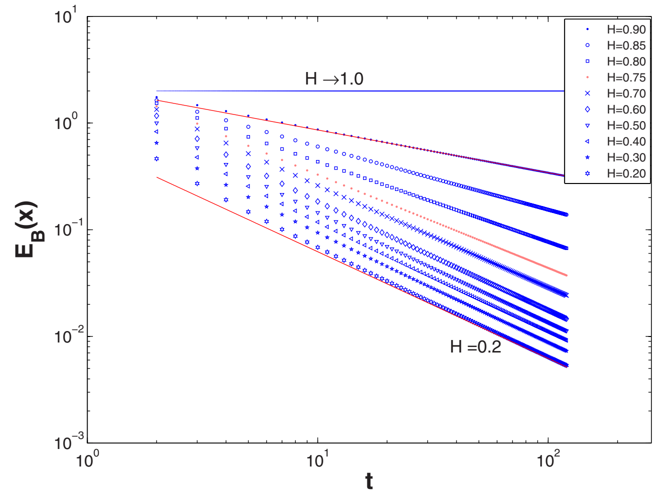

FIG. 2. (Color online) The E_B parameter Eq. (13) for fractional Brownian motion $x(t)$ versus time t, for different values of the Hurst exponent. Here we present exact results obtained directly by calculating Eqs. (10), (A3), and (A4). The two solid lines (red online) are the asymptotic theory Eq. (13) for $H=0.2$ and 0.9. In the ballistic limit $H \to 1$, we get nonergodic behavior. Notice that for $H<3/4$ and long t, the curves are parallel to each other due to the $E_B \sim t^{-1}$ law valid for $H<3/4$, while for $H>3/4$ the slopes are changing as we vary H. The lag time is $\Delta=1$.

the cell boundary. Direct comparison at this stage between experiments and stochastic theory is impossible, since the number of measured trajectories is small.

B. Overdamped fractional Langevin equation

We now analyze the overdamped fractional Langevin Eq. (7). We can rewrite it in a convenient way as

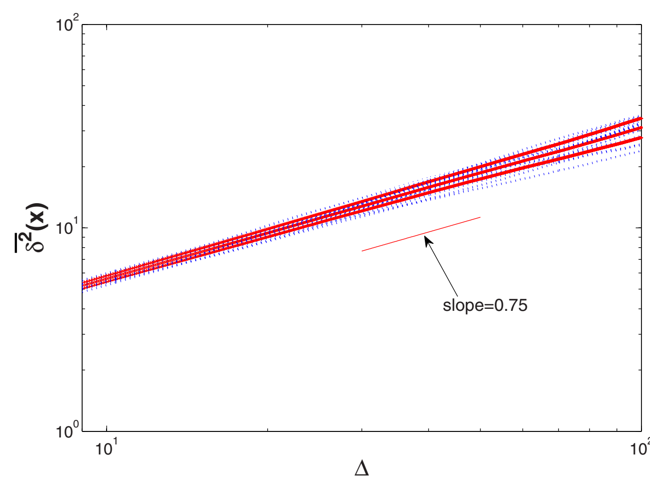

FIG. 3. (Color online) We simulate fBM and present the time average $\overline{\delta^2}(x(t))$ versus Δ (dotted curves, blue online). We show 23 trajectories, the solid line in the middle being the average of the trajectories. We observe $\overline{\delta^2}(x(t)) \propto \Delta^{3/4}$, similar to that in [11,12]. The measurement time is $t=10^4$, $H=\frac{3}{8}$, $D_H=\frac{1}{2}$. Line with a slope of 0.75 is drawn to guide the eye. We also show $\langle\overline{\delta^2}\rangle \pm \sqrt{X_{\rm var}(\overline{\delta^2})}$ (two solid lines, red online) obtained from Eqs. (10) and (A11), which give an analytical estimate on the scatter of the data.

$$\bar{\gamma}\Gamma(2H-1)D^{1-2H}Dz(t) = \eta\xi(t), \quad (15)$$

where $D=d/dt$, and D^{1-2H} is the Riemann-Liouville fractional integral of $2H-1$ order. Using the tools of fractional calculus [30], we get

$$\bar{\gamma}\Gamma(2H-1)z(t) = \eta D^{2H-2}\xi(t). \quad (16)$$

Then since $\langle\xi(t)\rangle=0$ we have $\langle z(t)\rangle=0$, and

$$\langle z(t_1)z(t_2)\rangle = D_F(t_1^{2-2H} + t_2^{2-2H} - |t_1 - t_2|^{2-2H}), \quad (17)$$

where

$$D_F = \frac{k_B T\pi \csc[\pi(2-2H)]}{\bar{\gamma}(2-2H)\Gamma^2(2H-1)\Gamma^2(2-2H)}.$$

From Eq. (17) we learn that Eq. (15) exhibits the same behavior as fBM [Eq. (2)] in the subdiffusion case. Note that for fBM $\langle x^2\rangle \sim t^\alpha$ with $\alpha=2H$ while for the fractional Langevin equation $\langle z^2\rangle \sim t^\alpha$ with $\alpha=2-2H$, and of course the diffusion constants have different dependencies on parameters of the noise. However, these minor modifications do not change our main result for $0<H<\frac{1}{2}$ obtained in the previous section (only switch the value $2H$ to $2-2H$). To see this, note that the E_B parameter depends on the behavior of correlation function Eq. (3) and the latter are identical for the processes $x(t)$ and $z(t)$ in the subdiffusion case, so $E_B(z) \sim E_B(x)$.

C. Underdamped fractional Langevin equation

We now analyze the fractional Langevin equation with power-law kernel, Eq. (6),

$$m\frac{d^2y(t)}{dt^2} = -\bar{\gamma}\int_0^t (t-\tau)^{2H-2}\frac{dy}{d\tau}d\tau + \eta\xi(t), \quad (18)$$

with $dy(0)/dt=v_0$, $y(0)=0$, where v_0 is the initial velocity. The solution of the stochastic Eq. (18) is

$$y(t) = v_0 t E_{2H,2}(-\gamma t^{2H}) + \frac{\eta}{m}\int_0^t (t-\tau) \times E_{2H,2}(-\gamma(t-\tau)^{2H})\xi(\tau)d\tau,$$

where $\gamma=[\bar{\gamma}\Gamma(2H-1)]/m$ and the generalized Mittag-Leffler function is

$$E_{\alpha,\beta}(t) = \sum_{n=1}^{\infty}\frac{t^n}{\Gamma(\alpha n+\beta)},$$

and $E_{\alpha,\beta}(-t) \sim [t\Gamma(\beta-\alpha)]^{-1}$ when $t\to+\infty$. We have

$$\langle y(t)\rangle = v_0 t E_{2H,2}(-\gamma t^{2H}) \sim \frac{v_0}{\gamma}\frac{t^{1-2H}}{\Gamma(2-2H)} \quad (19)$$

and

$$\langle y^2(t)\rangle = \frac{2k_BT}{m}t^2E_{2H,3}(-\gamma t^{2H}) \sim \frac{2k_BT}{\bar{\gamma}\Gamma(2H-1)\Gamma(3-2H)}t^{2-2H}, \quad (20)$$

where the thermal initial condition $v_0^2=k_BT/m$ is assumed. Note that for short times we have $\langle y^2(t)\rangle \sim (k_BT/m)t^2$. Equations (19) and (20) were found [32,33].

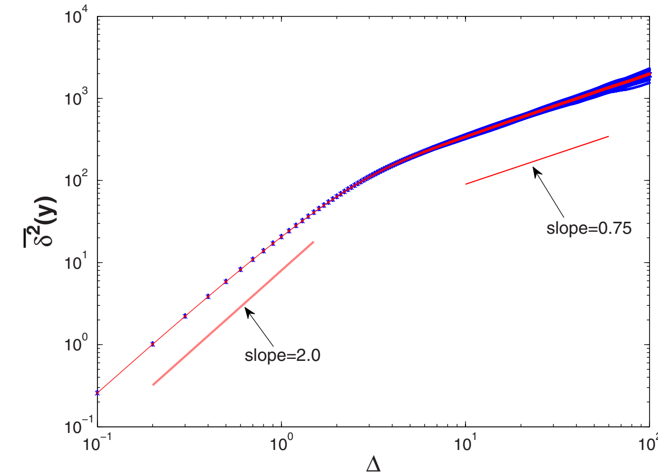

FIG. 4. (Color online) The time average $\overline{\delta^2}(y(t))$ is a random variable depending on the underlying trajectory. A total of 23 trajectories, besides the solid line, with ● denoting the average of the 23 trajectories, are plotted. The measurement time is $t=10^4$, $2-2H=0.75$, $D_H=\frac{1}{2}$, $m=1$, $\bar{\gamma}=1$, $v_0=1$, $k_BT=1$. Lines with slopes of 2.0 (ballistic motion in short times) and 0.75 (subdiffusion for long times) are drawn to guide the eye. For long Δ the behavior of the underdamped motion is similar to usual fractional Brownian motion.

The covariance of $y(t)$ reads

$$\langle y(t_1)y(t_2)\rangle = v_0^2 t_1 t_2 E_{2H,2}(-\gamma t_1^{2H})E_{2H,2}(-\gamma t_2^{2H}) + \frac{k_BT\bar{\gamma}}{m^2}\int_0^{t_2}\int_0^{t_1} d\tau ds(t_1-\tau)E_{2H,2}[-\gamma(t_1-\tau)^{2H}] \times(t_2-s)E_{2H,2}[-\gamma(t_2-s)^{2H}]|\tau-s|^{2H-2}. \quad (21)$$

When t_1,t_2 tend to infinity,

$$\langle y(t_1)y(t_2)\rangle \sim \frac{k_BT}{\bar{\gamma}\Gamma^2(2H-1)\Gamma^2(2-2H)}\int_0^{t_2}\int_0^{t_1} d\tau ds \times(t_1-\tau)^{1-2H}(t_2-s)^{1-2H}|\tau-s|^{2H-2}, \quad (22)$$

i.e., the covariance of $y(t)$ approximates to the ones of $z(t)$, so we can expect in the long-time limit

$$\langle\overline{\delta^2}(y)\rangle \sim \langle\overline{\delta^2}(z)\rangle \sim \langle\overline{\delta^2}(x)\rangle \quad (23)$$

and

$$E_B(y) \sim E_B(z) \sim E_B(x). \quad (24)$$

The simulations (see Appendix B for the computational scheme), Fig. 4, confirms Eq. (23), and Figs. 5 and 6 support Eq. (24). Note that for short times we have a ballistic behavior for $y(t)$ (see Fig. 4), but not for $z(t)$ and $x(t)$, so clearly both Δ and t must be large for Eq. (24) to hold.

IV. DISCUSSION

We showed that the fractional processes $x(t)$, $y(t)$, and $z(t)$ are ergodic. The ergodicity breaking parameter decays as a power law to zero. In the ballistic limit $\langle x^2\rangle \sim t^2$, nonergod-

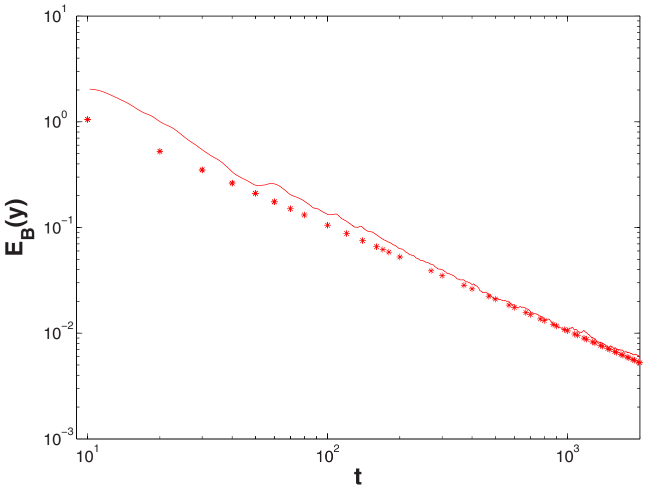

FIG. 5. (Color online) The ergodicity breaking parameter $E_B(y)$ versus t. Simulations of 200 trajectories were used with $2-2H=0.75$, $\Delta=10$, $m=1$, $\bar{\gamma}=1$, $v_0=1$, $k_BT=1$. The stars $*$ are the theoretical result Eq. (13) without fitting.

icity is found. For the opposite localization limit $\langle x^2\rangle \sim t^0$ (i.e., $H\to 0$ for fBM), the asymptotic convergence is reached only after very long times. Our most surprising result is that the transition between the localization limit and the ballistic limit is not smooth. When $H=\frac{3}{4}$, the behavior of the E_B parameter is changed and the amplitude $k(H)$ diverges [36].

Clearly anomalous diffusion is not a sufficient condition for ergodicity breaking. While the subdiffusive CTRW model [13] is nonergodic, the fBM and fractional Langevin motion are ergodic. Another important difference is that for an infinite system we have for the CTRW $\langle\overline{\delta^2}\rangle \sim \Delta/t^\alpha$, so the time-average procedure yields a linear dependence on Δ and an aging effect with respect to the measurement time. Hence for CTRW an anomalous diffusion process may seem normal with respect to Δ [13,14,37,38]. In contrast, for the fractional models we investigated here we have $\langle\overline{\delta^2}\rangle \sim \Delta^\alpha$, which is the same as the ensemble average $\langle x^2\rangle \sim t^\alpha$. The main difference between the two approaches is that the CTRW process is nonstationary.

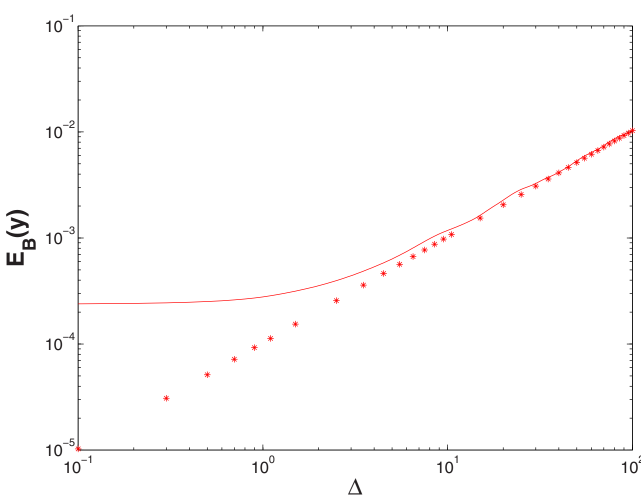

FIG. 6. (Color online) The ergodicity breaking parameter $E_B(y)$ versus Δ. A total of 200 trajectories are used to compute the average and variance, the measurement time $t=10^4$, $2-2H=0.75$, $m=1$, $\bar{\gamma}=1$, $v_0=1$, $k_BT=1$. The stars $*$ are the theoretical result Eq. (13) with corresponding parameter values. We see that results found from the underdamped Langevin equation converge to our analytical theory based on fBM.

Experiments in the cell are conducted for finite times, the main reason being the finite lifetime of the cell. Hence the whole physical concept of ergodicity might not be applicable, since in experiments we cannot perform long time averages. In finite-time experiments even normal processes may seem nonergodic and anomalous, and what may seem to be a deviation from ergodic behavior may actually be a finite-time effect. Here we gave analytical predictions for the deviations from ergodicity for finite-time measurement, based on three fractional models. The E_B parameter depends on measurement time and lag time, and can be used to compare experimental data with predictions of fractional equations. The E_B parameter for the CTRW is given in [13]. It should be noted, however, that for subdiffusion in the cell, the effects of the boundary of the cell, and three-dimensional trajectories, might be important. These effects should be investigated in the future, most likely with simulations. Further, as mentioned in the text, direct comparison between experiments and theory is not yet possible, since the number of measured trajectories is small.

ACKNOWLEDGMENTS

This work was supported by the Israel Science Foundation. W.D. was also partially supported by the National Natural Science Foundation of China under Grant No. 10801067. E.B. thanks S. Burov for discussions.

APPENDIX A: DERIVATION OF THE MAIN RESULT, EQ. (13)

From Eq. (10),

$$\langle[\overline{\delta^2}(x(t))]^2\rangle = \frac{\int_0^{t-\Delta} dt_1 \int_0^{t-\Delta} dt_2 \langle[x(t_1+\Delta)-x(t_1)]^2[x(t_2+\Delta)-x(t_2)]^2\rangle}{(t-\Delta)^2}. \tag{A1}$$

Using Eq. (3) and the following formula for Gaussian process with mean zero [31],

$$\langle x(t_1)x(t_2)x(t_3)x(t_4)\rangle = \langle x(t_1)x(t_2)\rangle\langle x(t_3)x(t_4)\rangle + \langle x(t_1)x(t_3)\rangle \times\langle x(t_2)x(t_4)\rangle + \langle x(t_1)x(t_4)\rangle\langle x(t_2)x(t_3)\rangle,$$

we obtain

$$\langle[x(t_1+\Delta)-x(t_1)]^2[x(t_2+\Delta)-x(t_2)]^2\rangle = 4D_H^2\Delta^{4H} + 2D_H^2\{|t_1+\Delta-t_2|^{2H}+|t_2+\Delta-t_1|^{2H}-2|t_1-t_2|^{2H}\}^2. \tag{A2}$$

From Eqs. (10), (11), (A1), and (A2), we have

$$X_{\rm var}[\overline{\delta^2}(x(t))] = \underbrace{4D_H^2\left\{\int_0^{2\Delta}(t-\Delta-t')\{(t'+\Delta)^{2H}+|t'-\Delta|^{2H}-2t'^{2H}\}^2 \mathrm{d}t'\right\}\bigg/(t-\Delta)^2}_{V_1} \tag{A3}$$

$$+\underbrace{4D_H^2\left\{\int_{2\Delta}^{t-\Delta}(t-\Delta-t')\{(t'+\Delta)^{2H}+(t'-\Delta)^{2H}-2t'^{2H}\}^2 \mathrm{d}t'\right\}\bigg/(t-\Delta)^2}_{V_2}. \tag{A4}$$

When $t \gg \Delta$, we may approximate the upper limit in the integral of V_2 with t, and $1/(t-\Delta)^2 \to 1/t$. We then make a change of variables according to $x=(t-t')/t$ and find

$$V_2 = 4D_H^2 t^{4H}\int_0^1 x(1-x)^{4H}\left[\left(1+\frac{\Delta}{t(1-x)}\right)^{2H} + \left|1-\frac{\Delta}{t(1-x)}\right|^{2H}-2\right]^2 \mathrm{d}x. \tag{A5}$$

We expand in Δ/t to second order and find

$$V_2 \sim 4D_H^2 t^{4H}\left(\frac{\Delta}{t}\right)^4 H^2(2H-1)^2\int_0^1 x(1-x)^{4H-4}\mathrm{d}x. \tag{A6}$$

The integral is finite only if $H>\frac{3}{4}$, hence for $H\leqslant\frac{3}{4}$ we will soon use a different approach. We see that $V_2 \sim t^{4H-4}$ while it is easy to show that $V_1 \sim 1/t$, hence for $H>\frac{3}{4}$ we find after solving the integral

$$X_{\rm var}[\overline{\delta^2}(x(t))] \sim 16D_H^2 t^{4H}\left(\frac{\Delta}{t}\right)^4 H^2(2H-1)^2\left(\frac{1}{4H-3}-\frac{1}{4H-2}\right). \tag{A7}$$

Now we write the variance as

$$X_{\rm var}[\overline{\delta^2}(x(t))] = \frac{4D_H^2}{(t-\Delta)^2}\int_0^{t-\Delta}(t-\Delta-t')[(t'+\Delta)^{2H} + |t'-\Delta|^{2H}-2t'^{2H}]^2\mathrm{d}t'. \tag{A8}$$

Changing variables according to $\tau=t'/\Delta$, we find

$$X_{\rm var}[\overline{\delta^2}(x(t))] = \frac{4D_H^2}{(t-\Delta)}\Delta^{4H+1}\int_0^{t/\Delta-1}\mathrm{d}\tau[(1+\tau)^{2H}+|1-\tau|^{2H} -2\tau^{2H}]^2 + X_{\rm corr}. \tag{A9}$$

The correction term is

$$X_{\rm corr} = -\frac{4D_H^2}{(t-\Delta)^2}\Delta^{4H+2}\int_0^{t/\Delta-1}\mathrm{d}\tau[(1+\tau)^{2H}+|1-\tau|^{2H} -2\tau^{2H}]^2\tau. \tag{A10}$$

Taking the upper limit of the integral in Eq. (A9) to ∞, we find that for $H<\frac{3}{4}$ and long times

$$X_{\rm var}[\overline{\delta^2}(x(t))] \sim 4D_H^2\Delta^{4H}\left(\frac{\Delta}{t}\right)\int_0^{\infty}\mathrm{d}\tau[(1+\tau)^{2H}+|1-\tau|^{2H} -2\tau^{2H}]^2. \tag{A11}$$

This is because $X_{\rm corr} \sim t^{\max\{4H-4,-2\}}$ (we prove this in the following) and this term is smaller than the leading term, which has a $1/t$ decay, since $H<\frac{3}{4}$. Now we estimate the correction term Eq. (A10),

$$\frac{1}{t^2}\int_0^{t/\Delta-1}\mathrm{d}\tau[(1+\tau)^{2H}+|1-\tau|^{2H}-2\tau^{2H}]^2\tau = \frac{1}{t^2}\left(\int_0^2 \mathrm{d}\tau + \int_2^{t/\Delta-1}\mathrm{d}\tau\right)[(1+\tau)^{2H}+|1-\tau|^{2H}-2\tau^{2H}]^2\tau. \tag{A12}$$

Using the Lagrange reminder of Taylor expansion in $1/\tau$, when $H\leqslant\frac{3}{4}$ we have

$$\begin{aligned}\frac{1}{t^2}\int_2^{t/\Delta-1}\mathrm{d}\tau[(1+\tau)^{2H}+|1-\tau|^{2H}-2\tau^{2H}]^2\tau &= \frac{1}{t^2}\int_2^{t/\Delta-1}\mathrm{d}\tau\left[\left(1+\frac{1}{\tau}\right)^{2H}+\left|1-\frac{1}{\tau}\right|^{2H}-2\right]^2\tau^{4H+1}\\ &= \frac{1}{t^2}\int_2^{t/\Delta-1}\mathrm{d}\tau[(1+\xi)^{2H-2}+(1-\xi)^{2H-2}]\\ &\quad\times 2H(2H-1)\tau^{4H-3}\quad \text{where}\quad \left(\xi\in\left[0,\tfrac{1}{2}\right]\right)\\ &\sim t^{\max\{4H-4,-2\}}.\end{aligned} \tag{A13}$$

For $H=\frac{3}{4}$ we use Eq. (A9), however now we expand to third order and find

$$X_{\text{var}}[\overline{\delta^2}(x(t))] \sim 16D_H^2H^2(2H-1)^2\Delta^3 \ln t\left(\frac{\Delta}{t}\right), \tag{A14}$$

while the correction term $X_{\text{corr}} \sim t^{-1}$ [see Eq. (A13)] is negligible. Using Eqs. (A7), (A11), and (A14), we derive Eq. (13).

APPENDIX B: COMPUTATIONAL SCHEME FOR EQ. (6)

The numerical algorithm for simulating the trajectories of the generalized Langevin equation is developed by combining the predictor-corrector method [5] with Hosking's approach (to generate fBM). The computational scheme is as follows [35]:

$$y_h(t_{n+1}) = y_0 + h\sum_{j=1}^{n} v_h(t_j) + h[v_0 + v_h(t_{n+1})]/2, \tag{B1}$$

where $dy(0)/dt = v_0$ and

$$v_h(t_{n+1}) = \left(\frac{2H(2H+1)m}{2H(2H+1)m + h^{2H}\bar{\gamma}}\right) \times \left(v_0 - \frac{h^{2H}}{2H(2H+1)}\frac{\bar{\gamma}}{m}\sum_{j=0}^{n} a_{j,n+1}v_h(t_j) + \frac{\eta}{m}B_H(t_{n+1})\right), \tag{B2}$$

with

$$a_{j,n+1} = \begin{cases} n^{2H+1} - (n-2H)(n+1)^{2H} & \text{if } j=0, \\ (n-j+2)^{2H+1} + (n-j)^{2H+1} - 2(n-j+1)^{2H+1} & \text{if } 1 \leqslant j \leqslant n, \end{cases} \tag{B3}$$

where h is the step length, i.e., $h = t_{j+1} - t_j$.

[1] R. Metzler and J. Klafter, Phys. Rep. **339**, 1 (2000).
[2] F. Mainardi and E. Bonetti, Rheol. Acta **26**, 64 (1988).
[3] R. Metzler, E. Barkai, and J. Klafter, Phys. Rev. Lett. **82**, 3563 (1999).
[4] E. Barkai, R. Metzler, and J. Klafter, Phys. Rev. E **61**, 132 (2000); E. Barkai, *ibid.* **63**, 046118 (2001).
[5] W. H. Deng, J. Comput. Phys. **227**, 1510 (2007); SIAM (Soc. Ind. Appl. Math.) J. Numer. Anal. **47**, 204 (2008).
[6] B. B. Mandelbrot and J. W. van Ness, SIAM Rev. **10**, 422 (1968).
[7] I. Goychuk and P. Hänggi, Phys. Rev. Lett. **99**, 200601 (2007).
[8] W. Min, G. Luo, B. J. Cherayil, S. C. Kou, and X. S. Xie, Phys. Rev. Lett. **94**, 198302 (2005).
[9] S. Burov and E. Barkai, Phys. Rev. Lett. **100**, 070601 (2008).
[10] W. T. Coffey, Yu. P. Kalmykov, and J. T. Waldron, *The Langevin Equation* (World Scientific, Singapore, 2004).
[11] I. Golding and E. C. Cox, Phys. Rev. Lett. **96**, 098102 (2006).
[12] I. M. Tolić-Nørrelykke, E. L. Munteanu, G. Thon, L. Oddershede, and K. Berg-Sorensen, Phys. Rev. Lett. **93**, 078102 (2004).
[13] Y. He, S. Burov, R. Metzler, and E. Barkai, Phys. Rev. Lett. **101**, 058101 (2008).
[14] A. Lubelski, I. M. Sokolov, and J. Klafter, Phys. Rev. Lett. **100**, 250602 (2008).
[15] I. M. Sokolov, Phys. **1**, 8 (2008).
[16] J. Saxton, Biophys. J. **72**, 1744 (1997).
[17] X. Brokmann, J. P. Hermier, G. Messin, P. Desbiolles, J. P. Bouchaud, and M. Dahan, Phys. Rev. Lett. **90**, 120601 (2003).
[18] G. Margolin and E. Barkai, Phys. Rev. Lett. **94**, 080601 (2005).
[19] A. Rebenshtok and E. Barkai, Phys. Rev. Lett. **99**, 210601 (2007).
[20] G. Bel and E. Barkai, Phys. Rev. Lett. **94**, 240602 (2005).
[21] J. D. Bao, P. Hänggi, and Y. Z. Zhuo, Phys. Rev. E **72**, 061107 (2005).
[22] M. H. Lee, Phys. Rev. Lett. **87**, 250601 (2001).
[23] I. V. L. Costa, R. Morgado, M. V. B. T. Lima, and F. A. Oliveira, Europhys. Lett. **63**, 173 (2003).
[24] I. V. L. Costa *et al.*, Physica A **371**, 130 (2006).
[25] A. Dhar and K. Wagh, Europhys. Lett. **79**, 60003 (2007).
[26] A. V. Plyukhin, Phys. Rev. E **77**, 061136 (2008).
[27] S. C. Lim and S. V. Muniandy, Phys. Rev. E **66**, 021114 (2002).
[28] G. Samorodnitsky and M. Taqqu, *Stable Non-Gaussian Random Processes: Stochastic Models with Infinite Variance* (Chapman and Hall, New York, 1994).
[29] R. Kupferman, J. Stat. Phys. **114**, 291 (2004).
[30] C. P. Li and W. H. Deng, Appl. Math. Comput. **187**, 777 (2007).
[31] R. Kubo, M. Toda, and N. Hashitsume, *Statistical Physics II: Nonequilibrium Statistical Mechanics* (Springer-Verlag, Heidelberg, 1995).
[32] E. Lutz, Phys. Rev. E **64**, 051106 (2001).
[33] E. Barkai and R. J. Silbey, J. Phys. Chem. B **104**, 3866 (2000).
[34] J. R. M. Hosking, Water Resour. Res. **20**, 1898 (1984).
[35] A detailed derivation of the numerical scheme and error and stability analysis will be presented in an upcoming publication.
[36] Other very different critical exponents of fractional Langevin equations were recently found in [9]. There the critical exponents mark transitions between overdamped and underdamped motion. So stochastic fractional processes possess a large number of critical exponents.
[37] E. Barkai and Y. C. Cheng, J. Chem. Phys. **118**, 6167 (2003).
[38] E. Barkai, Phys. Rev. Lett. **90**, 104101 (2003).